NASA Technical Memorandum 104355

Modeling of Crack Bridging in a Unidirectional Metal Matrix Composite

Louis J. Ghosn
Sverdrup Technology Inc.
Lewis Research Center Group
Brook Park, Ohio

and

Pete Kantzos and Jack Telesman
National Aeronautics and Space Administration
Lewis Research Center
Cleveland, Ohio

May 1991

NASA

MODELING OF CRACK BRIDGING IN A UNIDIRECTIONAL METAL MATRIX COMPOSITE

Louis J. Ghosn
Sverdrup Technology, Inc.
Lewis Research Center Group
Brook Park, Ohio 44142

Pete Kantzos, and Jack Telesman
National Aeronautics and Space Administration
Lewis Research Center
Cleveland, Ohio 44135

ABSTRACT

The effective fatigue crack driving force and crack opening profiles were determined analytically for fatigue tested unidirectional composite specimens exhibiting fiber bridging. The crack closure pressure due to bridging was modeled using two approaches; the fiber pressure model and the shear lag model. For both closure models, the Bueckner weight function method and the finite element method were used to calculate crack opening displacements and the crack driving force. The predicted near crack tip opening profile agreed well with the experimentally measured profiles for single edge notch SCS-6/Ti-15-3 metal matrix composite specimens. The numerically determined effective crack driving force, ΔK_{eff}, was calculated using both models to correlate the measured crack growth rate in the composite. The calculated ΔK_{eff} from both models accounted for the crack bridging by showing a good agreement between the measured fatigue crack growth rates of the bridged composite and that of unreinforced, unbridged titanium matrix alloy specimens.

SYMBOLS

a	total crack length
a_0	initial machined crack length
b	specimen thickness
c(x)	closure pressure
E_c	composite modulus
E_f	fiber modulus

E_m	matrix modulus
H(a,x)	Bueckner Weight function
K(a)	homogenized composite stress intensity factor
K_{st}	nonlinear foundation constant
m_1, m_2	geometrical constants
P(x')	net applied stress
R	fiber radius
R ratio	stress ratio, $(\sigma^{\infty}_{min}/\sigma^{\infty}_{max})$
u(x)	crack opening displacement
v_f	fiber volume fraction
w	specimen width
x	distance from the free edge
x'	dummy integration variable
Δa	crack increment $(a - a_0)$
ΔK	composite stress intensity range
ΔK_{app}	applied stress intensity range assuming no fiber bridging
ΔK_{eff}	effective stress intensity range in the matrix
ΔK_{th}	matrix threshold stress intensity factor range
Δu	crack opening displacement range $(u_{max} - u_{min})$
$\Delta\sigma^{\infty}$	applied stress range $(\sigma^{\infty}_{max} - \sigma^{\infty}_{min})$
ν_c	composite poisson's ratio
τ	fiber/matrix interfacial frictional shear stress
σ^{∞}	applied remote stress
ℓ	dummy integration variable

INTRODUCTION

The new generation of aerospace vehicles will require low density/high strength materials capable of withstanding high temperatures while retaining a high stiffness

under relatively high loads. Continuous fiber, metal matrix composites (MMC) are candidate materials for such applications.

The ability to predict fatigue crack growth behavior of these composites is of particular interest due to the presence of many crack-like defects in these materials. Experimental studies on a number of these composites (Refs. 1,2) have shown that cracks tend to propagate in the metallic matrix leaving behind unbroken fibers which bridge the cracked surfaces. Unbroken fibers in the wake of the crack carry some of the applied load and thus shield the crack tip. As the crack grows, the bridging zone increases and further shields the crack tip by reducing the overall crack driving force (Ref. 2).

A number of researchers (Refs. 3-9) have attempted to model crack bridging. The crack bridging model that has received the most attention for composite materials is the so-called shear lag model (SLM) (Refs. 3-6). This model is based on the relative sliding between the fiber and the matrix in the region where the interface shear stresses exceed the strength of the interface. This model was developed for brittle matrix fiber composites with only a frictional constrain between the fibers and the matrix. Recently this model has also been applied to metal matrix composites exhibiting fiber bridging (Ref. 4).

Another type of bridging model which may be applicable for these types of composites is based on the application of a closure pressure in the bridged zone proportional to the load carried by the bridging fibers (henceforth this model will be termed fiber pressure model (FPM)). This methodology had been applied previously to model the effect of unbroken ligaments in dynamic fracture testing of steels (Ref. 8) but has not been previously applied to composites or to fatigue modeling.

In order to decide how accurately these models represent the actual fatigue crack growth behavior, the predicted results from both models are compared to experimental test data obtained from single edge notch SCS-6/Ti-15-3 MMC specimens. Testing was performed using a specially designed loading stage mounted inside a SEM

(Ref. 10). The high magnification viewing of a specimen loaded inside a SEM permits accurate measurements of the crack opening displacements and of the crack growth rates.

CLOSURE MODELS

The effect of fibers bridging the crack faces can be modeled by applying a closure pressure in the bridged region as shown in Fig. 1. Different forms of closure pressures can be formulated depending on the fiber, matrix and interface properties (Ref. 9). The closure pressure formulation most commonly applied is the shear lag model (SLM) proposed by Marshall, Cox and Evans (Ref. 3). In their formulation, the closure pressure in the bridged region is a function of the fiber/matrix interfacial friction shear stress and is proportional to the square root of the opening displacement. The closure pressure is given by:

$$c(x) = 2\left(\frac{u(x)\tau v_f^2 E_f E_c}{R(1 - v_f)E_m}\right)^{1/2} \tag{1a}$$

where

$u(x)$ crack opening displacement

τ fiber/matrix interfacial frictional shear stress

E_c composite modulus

E_f fiber modulus

E_m matrix modulus

R fiber radius

v_f fiber volume fraction

Since $c(x)$ is a function of the unknown opening displacements, an iterative scheme is required to solve for these displacements.

Recently the closure pressure formulation in the shear lag model has been modified by McCartney (Ref. 11) to make the model energetically consistent. The new formulation is as follows:

$$c(x) = 2\left(\frac{u(x)\tau v_f^2 E_f E_c^2}{R(1 - v_f)^2 E_m^2}\right)^{1/2} \tag{1b}$$

In this study the original formulation of the closure pressure was used. The effect the new formulation would have had on the calculated results is discussed later on.

As an alternative to the shear lag model, the closure pressure in the fiber pressure model (FPM) is assumed to be equal to the stress carried by the fibers in the bridged region averaged out over the total bridged area $(a - a_0)$. The closure pressure $c(x)$ is given by:

$$c(x) = \sigma^{\infty}\left(\frac{w}{w - a_0} + \frac{6wa_0[0.5(w - a_0) - (x - a_0)]}{(w - a_0)^3}\right) \tag{2}$$

where σ^{∞} is the applied remote stress, w the width of the specimen, and a_0 and a are the initial notch length and the total crack length, respectively, and where x is the distance to the bridged area measured from the free surface. Equation (2) represents the normal and bending stresses in the bridged fiber region and is valid only for a partially bridged crack. This formulation is applicable to a composite system with very stiff fibers as in the case of MMC's with ceramic fibers.

Either the Bueckner weight function method or the finite element method can be used with the closure models to determine the effective stress intensity factor, ΔK_{eff}, and the crack opening profile. The formulation and application of each model are described in the following sections.

Bueckner Weight Function

The most direct method to determine the stress intensity factor and the crack opening profile is the weight function method. The weight function used is based on the Bueckner formulation (Ref. 12) for the stress intensity factor calculation of a single edge notch specimen with a finite geometry (Fig. 1(b)). This formulation

differs somewhat from the original formulation by Marshall, Cox and Evans of the shear lag model (Ref. 3) in that their weight function was for a crack in an infinite region.

The homogenized composite stress intensity factor for a partially bridged specimen is given by:

$$K(a) = \sqrt{\frac{2}{\pi}}\left(\int_0^{a_0} \frac{\sigma^{\infty} H(a,x')}{\sqrt{a - x'}}\, dx' + \int_{a_0}^{a} \frac{[\sigma^{\infty} - c(x')]H(a,x')}{\sqrt{(a - x')}}\, dx'\right) \tag{3}$$

where

$$H(a,x') = 1 + m_1\frac{a - x'}{a} + m_2\frac{(a - x')^2}{a^2} \tag{4}$$

and where m_1 and m_2 are a function of the ratio of the crack length over the width of the specimen and given by:

$$m_1 = 0.6147 + 17.1844\frac{a^2}{w^2} + 8.7822\frac{a^6}{w^6} \tag{5}$$

$$m_2 = 0.2502 + 3.2889\frac{a^2}{w^2} + 70.0444\frac{a^6}{w^6} \tag{6}$$

The Bueckner weight function method was extended to calculate the crack opening displacements. The crack opening displacements are calculated at a location x due to a crack extending from x to a. By varying the location of x over the entire crack length, the crack opening profile is obtained. The displacement at a location x is given by:

$$u(x) = \frac{2\left(1 - \nu_c^2\right)}{E_c\pi}\left\{\int_x^a \frac{H(\ell,x)}{\sqrt{\ell - x}}\left[\int_0^1 \frac{P(x')H(\ell,x')}{\sqrt{\ell - x'}}\, dx'\right] d\ell\right\} \tag{7}$$

where

$$P(x') = \begin{bmatrix} \sigma^{\infty} & \text{for } 0 < x' < a_0 \\ \sigma^{\infty} - c(x') & \text{for } a_0 < x' < a \end{bmatrix} \tag{8}$$

and where E_c and ν_c are the homogenized composite elastic modulus and Poisson's ratio, respectively in the loading direction.

Up to this point the analytical solution is identical for both closure models. The difference in the solution is due to the substitution of the appropriate closure pressure $c(x)$ for each model into Eqs. (3) and (7). For the fiber pressure model, a direct numerical integration of the equations gives the solution for the opening profile and the stress intensity factor. For the shear lag model, an iterative scheme is required with a small damping factor to guarantee convergence. The convergence of this method was rather slow and used substantial CPU time. To limit the CPU time, a finite element approach was also used to calculate the crack opening displacements and the crack driving force in the composite.

Finite Element Approach

The fiber pressure model was used in the finite element program as a nonuniform pressure applied in the bridged region. For the shear lag model, the closure pressure was applied as a nonlinear foundation pressure. Thus the closure pressure for the shear lag model is given by:

$$c(x) = K_{st}(u)u(x) \tag{9}$$

where $K_{st}(u)$ is a nonlinear foundation constant given by:

$$K_{st}(u) = 2\left(\frac{\tau v_f^2 E_f E_c}{u(x)R(1 - v_f)E_m}\right)^{1/2} \tag{10}$$

The finite element mesh used is shown in Fig. 2 for half the specimen, accounting for symmetry. Eight-noded quadrilateral plane strain elements were used with quarter

point singularity at the crack tip (Ref. 13). Finally, the composite stress intensity factor was determined from the displacement field near the crack tip. For simplicity, the FEM analysis utilized an isotropic only solution which is consistent with the Bueckner weight function formulation.

The advantage of the FEM over the Bueckner weight function method was the convergence speed for the shear lag model. The finite element solution for the shear lag model converged rapidly. After it was determined that both techniques produce very similar results, the rest of the analysis was performed using the Bueckner weight function method for the fiber pressure model and the finite element method for the shear lag model.

EXPERIMENTAL

A fatigue crack growth study was conducted on two single edge notch (SEN) metal matrix composite specimens. The test material was a SiC (SCS-6) fiber reinforced composite with a Ti-15V-3Cr-3Al-3Sn (Ti-15-3) matrix. The fiber diameter was 145 μm and the fiber volume fraction was 0.36. The testing was performed on unidirectionally oriented specimens with the fiber direction being parallel to the loading axis and perpendicular to the starter notch. The maximum stress applied for specimen number 1 was 220 MPa and 310 MPa for specimen number 2 (see Table 1). Both of the tests were performed at room temperature with an R ratio (minimum stress/ maximum stress) equal to 0.1 and a test frequency of 5 Hz. Composite specimens were tested inside a specially designed loading stage mounted inside a SEM (Ref. 10). Testing was periodically interrupted to measure the crack growth rates and crack opening displacements. The measurements were performed at high magnifications (up to 2000X). Crack opening displacements were measured both at the maximum and minimum applied stresses in order to obtain crack opening displacement range (Δu). Companion testing was performed on compact tension (CT) specimens machined out of unreinforced matrix alloy which was processed in a similar manner as the composite. Complete details of the testing program have been published in Ref. 2.

RESULTS AND DISCUSSION

Experimental Results

The fatigue crack growth results for the MMC specimens and the unreinforced matrix specimens tested are shown in Fig. 3. The fatigue crack growth behavior of the composite and the unreinforced matrix is drastically different. The behavior of the unreinforced matrix shows traditional fatigue crack growth characteristics. However, in the composite the crack growth rates of the MMC specimens were orders of magnitude lower than the unreinforced matrix specimens. In addition, the crack growth rates of the composite decreased with an increase in the crack length until an eventual crack arrest was achieved. The SEM observations revealed that the crack propagated only in the matrix leaving behind unbroken fibers to bridge the crack.

The effect of fiber bridging on the crack driving force and crack opening displacements was analyzed using the previously mentioned models and is described next.

Unbridged Single Edge Notch Specimen

To check the accuracy of the numerical integrations of the Bueckner weight function and the FEM analysis, the stress intensity factor (SIF) and the crack opening profile for an unbridged SEN specimen were first determined and compared with published results (Ref. 14). The results shown in Table 2, exhibit a very good agreement between the published results and those obtained through both type of analyses.

Crack Opening Displacements

The effect of fiber bridging on crack opening displacement in the SCS-6/Ti-15-3 metal matrix composite system was determined analytically using the fiber pressure model and the shear lag model. The values of the material properties and specimen parameters used for the analyses are given in Table 1 for the two testing conditions.

The crack opening displacement range, (Δu), data obtained using the shear lag model for different values of τ is plotted in Fig. 4 for a stress range of 198 MPA

and a crack length of 1.89 mm. Also plotted in Fig. 4 are the results from actual measurements of the displacement ranges obtained from the first specimen. The shear lag model with a τ value of approximately 20 MPa correlated well with the experimental results near the crack tip. As seen from the figure, the crack opening profile obtained by the shear lag model decreases with increasing τ.

It has proven to be rather difficult to accurately determine τ experimentally. The reported τ values for the SCS-6/Ti-15-3 range from ~5 to ~140 MPa (Refs. 15-18). While a τ of 20 MPa is on the lower end of the reported spectrum, it is still within the range of the reported values. It should be pointed out that the τ value calculated depends on the shear lag formulation used, Eq. (1a) versus Eq. (1b).

The Δu results calculated by the fiber pressure model and the shear lag model with a τ = 20 MPa are compared in Fig. 5 to the experimentally obtained measurements for both specimens tested. Shown in the figure are three sets of predictions versus actual measurements for three different combinations of applied load and crack length. For all three sets of data, both models predicted closely the experimentally obtained displacement range near the crack tip. However, for specimen number 1 (Fig. 5(a)), further away from the crack tip the actual Δu's are higher than those calculated by both closure models. This discrepancy near the machined notch root may be due to fibers and interfaces damaged during machining which would tend to increase the actual COD displacements. However, it should be pointed out that it is the near crack tip displacements that control the crack growth behavior, and both models predicted these displacements accurately.

Stress Intensity Factor

Both models were used to calculate a bridging corrected crack driving force, ΔK_{eff}. Since the cracking observed in the composite material tested was limited to the matrix only, the effective crack driving force is assumed to be the effective

stress intensity factor in the matrix of the composite. Assuming a condition of iso-strain between the composite constituents ahead of the crack tip, the effective crack driving force in the composite is related to the ΔK of the homogenized composite (obtained from Eq. (3)) by:

$$\Delta K_{eff} = \frac{\Delta K E_m}{E_c} \tag{11}$$

The effective stress intensity factor, K_{eff}, was calculated for the shear lag model as a function of applied stress for different values of τ. As shown in Fig. 6, at a given stress level, the calculated K_{eff} decreases with increasing τ. The effective crack driving force for the composite, ΔK_{eff}, is calculated from Fig. 6 by subtracting the K_{eff} at the minimum stress from the K_{eff} at the maximum stress. For further analysis using the shear lag model, τ with a value of 20 MPa was used since this value of τ resulted in the best description of the measured crack opening displacements.

Figure 7 shows the relationship between the crack driving force parameter, ΔK_{eff}, and the length of the crack over which bridging is occurring. The results shown are for both the fiber pressure and shear lag models. For comparison purposes, the applied stress intensity factor ΔK_{app} as a function of the crack length for the unbridged case is also shown. The unbridged analyses show an increase in the fatigue crack driving force with an increase in the crack length. On the other hand, both closure models show a decrease of ΔK_{eff} with an increase in the bridged crack length. The decrease in the ΔK_{eff} occurs at faster rate initially (until a crack extension, Δa, of approximately 0.25 mm is reached), after which the decrease in the ΔK_{eff} continues, albeit at a significantly lower rate. The 0.25 mm crack extension during which most of the decrease in the ΔK_{eff} occurred, corresponds to crack growth through two fiber rows. These results point to the rapid effect fiber bridging has on decreasing the crack driving force.

The models also predict an eventual crack arrest which was shown to occur experimentally. Once enough fibers bridged the crack wake to lower the ΔK_{eff} below the matrix alloy threshold level ΔK_{th}, crack arrest occurred.

The experimentally obtained composite FCG data is then plotted as a function of the effective crack driving force, ΔK_{eff}, as calculated by the closure models. The results are shown in Fig. 8, together with the MMC and unreinforced matrix alloy data plotted in terms of applied stress intensity factor ΔK_{app}. The calculated ΔK_{eff}, for both closure models, moved the MMC crack growth data into agreement with the crack growth trends exhibited by the unreinforced matrix alloy. Thus both models were able to account for the reduction in the stress intensity range in the matrix caused by the fiber bridging.

Couple trends exhibited by the data should be noted. For both specimens tested, the ΔK_{eff} calculated by the fiber pressure model was lower than the ΔK_{eff} obtained from the shear lag mode. Also in the case of the shear lag model, the ΔK_{eff} values for the specimen tested at $\Delta\sigma^{\infty}$ = 280 MPa were higher than those at $\Delta\sigma^{\infty}$ = 198 MPa and are further away from the data trends exhibited by the unreinforced matrix alloy.

McCartney (Ref. 11) reformulated Eq. (11) to calculate ΔK_{eff}. The new formulation, which takes into consideration the energy balance is as follows:

$$\Delta K_{eff} = \Delta K \left[\frac{E_m}{E_c(1 - V_f)} \right]^{1/2} \tag{12}$$

The crack growth data for both closure models was plotted in terms of McCartney's reformulated ΔK_{eff} parameter and is shown in Fig. 9. As seen in the figure, there is still a good agreement between the trends exhibited by the unreinforced matrix alloy specimens and the predictions made by the fiber pressure model. In case of the shear lag model, the new formulation of ΔK_{eff} shifted the predictions somewhat away

from the unreinforced matrix alloy data especially for the specimen tested at the higher stress level.

Comparison Between the Closure Models

As was described previously, both models were successful in predicting the crack opening displacements and accounting for the effect of fiber bridging on the composite fatigue crack growth data in terms of a crack driving force parameter, ΔK_{eff}. However, for this particular study the fiber pressure model offers certain advantages over the shear lag model. One advantage is in the direct method of determining the closure pressure, no iterative solutions are required to determine the crack opening profile and the computing time is much shorter in comparison to the shear lag model. Also, for the fiber pressure model, the material and specimen parameters needed to perform the calculations can be obtained through standard means. On the other hand, the shear lag model requires previous knowledge of the interfacial frictional shear stress. Even though this is the most crucial parameter required for modeling the MMC crack growth behavior by the shear lag approach, no standard method exists for obtaining this parameter. It has been shown that different methods used in obtaining a value of τ can result in markedly different results (Refs. 4,15-18). Only through a trial and error process and our unique capability of measuring crack opening profile, we were able to settle on a τ value which successfully predicted the test results.

As mentioned previously, the formulation to determine the closure pressure c(x) for the shear lag model has recently been reformulated (Eq. (1b)). With the new formulation, in order to obtain the same crack opening profile, the interfacial frictional shear stress, τ, has to be reduced by a factor of 3.2. This results in an operative τ of 6.2 MPa. This value of τ is on the lowest end of reported values for the SCS-6/Ti-15-3 composite and brings to question the use of the reformulated model to accurately predict crack bridging induced behavior.

While the use of the fiber pressure model is limited to the case of a partially bridged crack, it is very straightforward in its use and it did more than an adequate job in modeling the fatigue crack growth behavior of this particular composite.

SUMMARY

A study was performed to model the effect of fiber bridging on the fatigue crack driving force and crack opening displacements in a SCS-6/Ti-15-3 metal matrix composite. The bridging mechanism was modeled using the shear lag and fiber pressure models. Both the finite element method and the Bueckner weight function methods were used for each model to obtain the numerical solutions. The experimental segment of the study was performed in a specially designed fatigue loading stage mounted inside a scanning electron microscope which allowed for high magnification measurements of the crack opening displacements.

For both models, the predicted crack tip opening profile agreed very well with the experimentally obtained data. In the case of the shear lag model, use of the interfacial frictional shear stress of 20 MPa resulted in the best fit for the crack opening displacements. This value of τ remained constant for variations in $\Delta\sigma^{\infty}$ and crack length.

The numerically determined effective crack driving force, ΔK_{eff}, was calculated using both models to correlate the measured crack growth rates in the composite. The calculated ΔK_{eff} from both models accounted for crack bridging by showing a good agreement between the measured crack growth rates of the bridged composite and that of unreinforced, unbridged titanium matrix alloy specimens.

Even though both models showed excellent capability of predicting the effect of crack bridging on crack growth behavior, the fiber pressure model offers certain advantages over the shear lag model. The fiber pressure model is straightforward and requires considerably less computing time than the shear lag model. Probably the most important disadvantage of the shear lag model is the requirement to accurately

determine the interfacial frictional shear stress of the composite in question. This parameter, which is not required for the fiber pressure model, has been shown to be very difficult to obtain reliably.

REFERENCES

1. T.P. Gabb, J. Gayda, and R.A. Mackay, J. Compos. Mater. (1990) 667-686.
2. P. Kantzos, J. Telesman, and L.J. Ghosn, Fatigue Crack Growth in a Unidirectional SCS-6/Ti-15-3 Composite, presented at the 3rd Symposium on Composite Materials: Fatigue and Fracture, Orlando, FL, (1989) ASTM STP-1110, in press. (Also, NASA TM-103095.)
3. D.B. Marshall, B.N. Cox, and A.G. Evans, Acta Metall. 33 (1985) 2013-2021.
4. M.D. Sensmeier, and P.K. Wright, in Fundamental Relationships Between Microstructures and Mechanical Properties of Metal Matrix Composites, P.K. Liaw and M.N. Gungor, eds., TMS, Warrendale, PA (1990) 441-457.
5. A.G. Evans and R.M. McMeeking, Acta Metall. 34 (1986) 2435-2441.
6. D.B. Marshall, and B.N. Cox, Acta Metall. 35 (1987) 2607-2619.
7. B. Budiansky, and J.C. Amazigo, J. Mech. Phys. Solids 37 (1989) 93-109.
8. R.G. Hoagland, A.R. Rosenfield, and G.T. Hahn, Met. Trans. 3 (1972) 123-136.
9. L.R.F. Rose, J. Mech. Phys. Solids 35 (1987) 383-405.
10. J. Telesman, P. Kantzos, and D. Brewer, in Lewis Structures Technology-1988, NASA CP-3003, Vol. 3 (1988) 161-172.
11. L.N. McCartney, Proc. R. Soc. Lond. A 409 (1987) 329-350.
12. H.F. Bueckner, Z. Angew. Math. Mech. 51 (1971) 97-109.
13. R.S. Barsoum, Int. J. Numer. Meth. Eng. 10 (1976) 25-38.
14. H. Tada, P.C. Paris, and G.R. Irwin, The Stress Analysis of Cracks Handbook, 2nd edition, Paris Productions, Inc., St. Louis, 1985.
15. M.R. James, private communication (1990).
16. C.J. Yang, S.M. Jeng, and J.M. Yang, Scr. Met. Mater. 24 (1990) 469-474.

17. B.M. Hillberry and W.S. Johnson, in Symposium on Micro-Cracking Induced Damage in Composites, Dallas, TX, ASME (1990) in publication. (Also, NASA TM-102751.)

18. P. Kantzos, unpublished work (1990).

TABLE 1. - SiC/Ti-15-3 METAL MATRIX COMPOSITE PROPERTIES AND TESTING CONDITIONS

	Specimen no. 1	Specimen no. 2
Unbridged length, mm	a_0 = 1.0	1.0
Specimen width, mm	w = 5.12	5.09
Specimen thickness, mm	b = 2.03	1.91
Maximum applied stress, MPa	σ^∞ = 220	311
Minimum applied stress, MPa	σ^∞ = 22	31
R ratio	0.1	0.1
Fiber modulus, GPa	E_f = 427	
Matrix modulus, GPa	E_m = 89	
Composite modulus, $[0]_8$, GPa	E_c = 184	
Composite Poisson's ratio, $[0]_8$	ν_c = 0.2825	
Fiber radius, μm	R = 72.5	
Fiber volume fraction	v_f = 0.36	

TABLE 2. - COMPARISON OF CRACK OPENING DISPLACEMENTS AND STRESS INTENSITY FACTORS FOR DIFFERENT ANALYTICAL METHODS FOR AN UNBRIDGED CRACK

(a/w = 0.37)

	Normalized displacement*	Normalized SIF
	$\frac{u(o)E}{4\sigma^\infty a}$	$\frac{K}{\sigma^\infty(\pi a)^{1/2}}$
Bueckner weight function	2.701	1.953
Finite element method	2.704	1.895
Tada (ref. 14)	2.675	1.957

*- at the free edge.

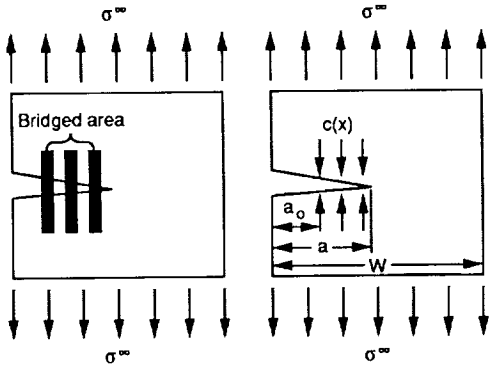

(a) Actual bridged crack. (b) Modeling of bridging using a closure pressure.

Figure 1.—Partially bridged single notch specimen.

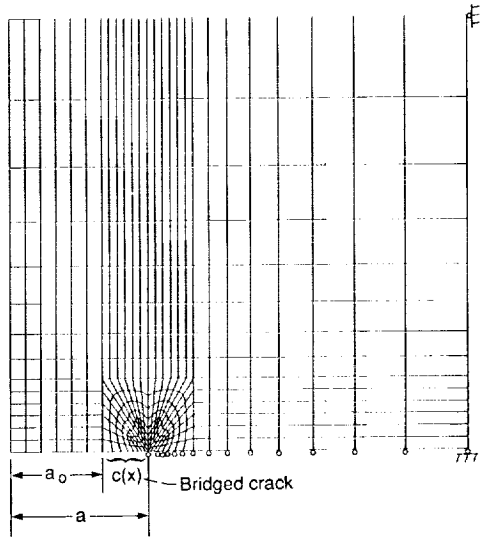

Figure 2.—Finite element mesh for single edge notch specimen.

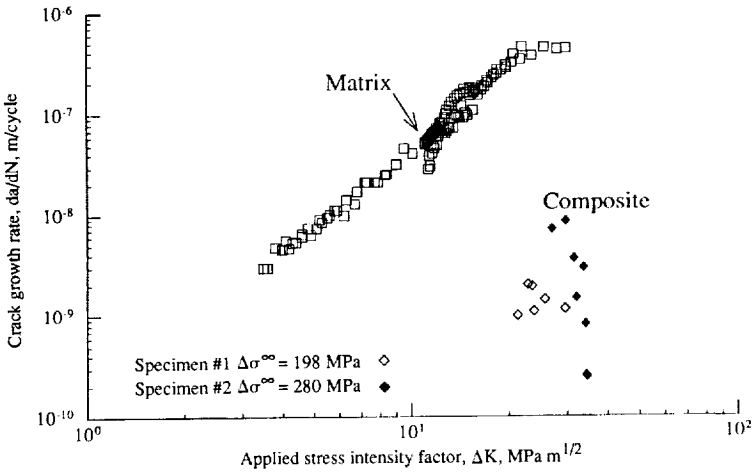

Figure 3.–Fatigue crack growth rates of the composite and the unreinforced matrix alloy specimens as a function of ΔK_{app}.

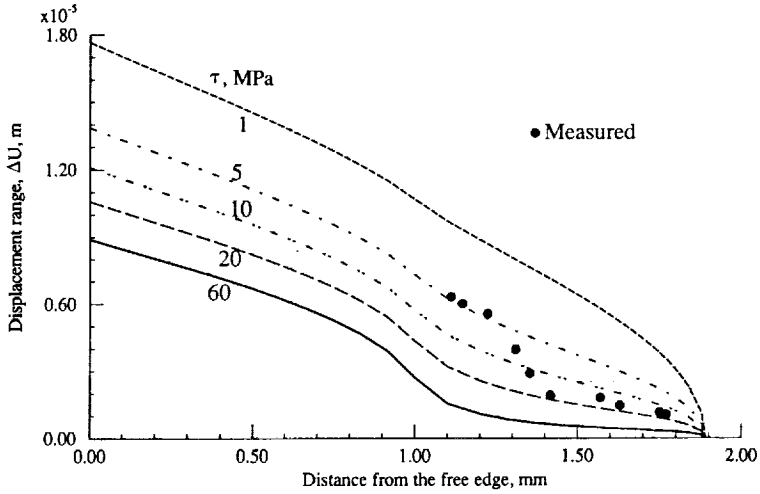

Figure 4.–Comparison of the measured crack opening displacement range with the shear lag model predictions for different values of the interfacial frictional shear stress τ. (a = 1.89 mm, $\Delta\sigma^{\infty}$ = 198 MPa, specimen #1.)

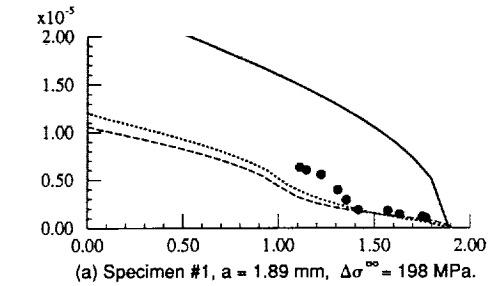

(a) Specimen #1, a = 1.89 mm, $\Delta\sigma^{\infty}$ = 198 MPa.

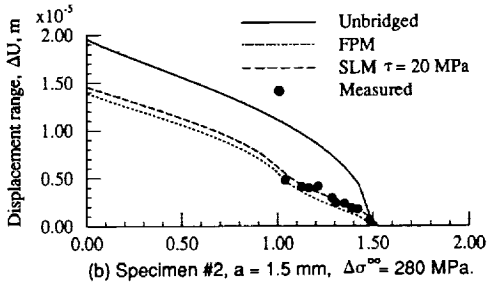

(b) Specimen #2, a = 1.5 mm, $\Delta\sigma^{\infty}$ = 280 MPa.

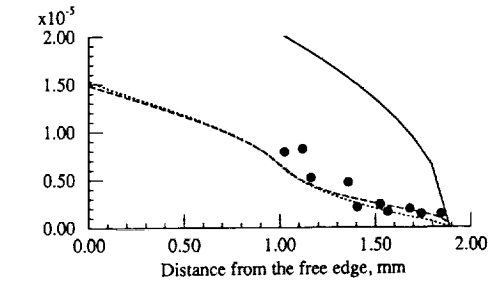

(c) Specimen #2, a = 1.89 mm, $\Delta\sigma^{\infty}$ = 280 MPa.

Figure 5.–Comparison of the measured ΔU profiles with the predicted profiles using the fiber pressure model and the shear lag model (τ = 20 MPa).

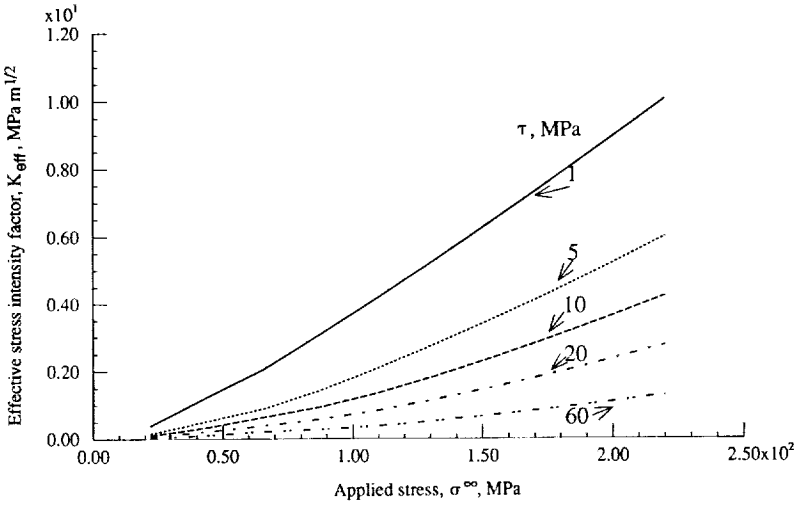

Figure 6.–The influence of the interfacial frictional shear stress on the effective stress intensity factor as a function of the applied stress for the shear lag model. (a = 1.89 mm, $\Delta\sigma^{\infty}$ = 198 MPa, specimen #1.)

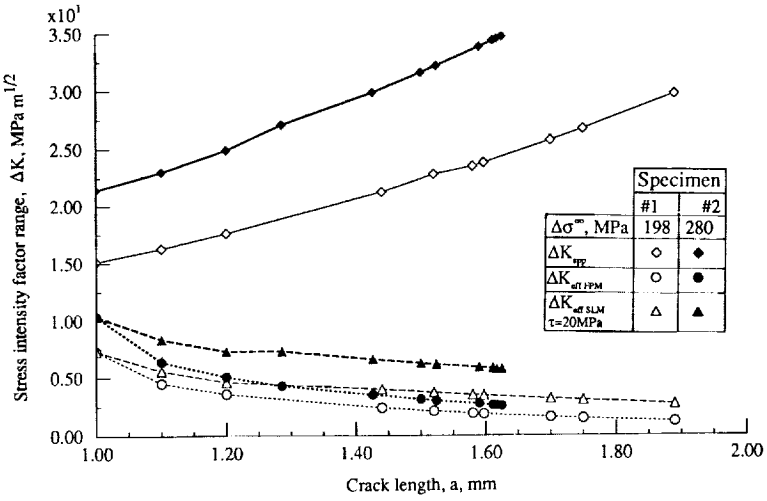

Figure 7.–Comparison between ΔK_{app} (unbridged) and ΔK_{eff} as a function of the crack length. ΔK_{eff} calculated using the fiber pressure model and the shear lag model (τ = 20 MPa).

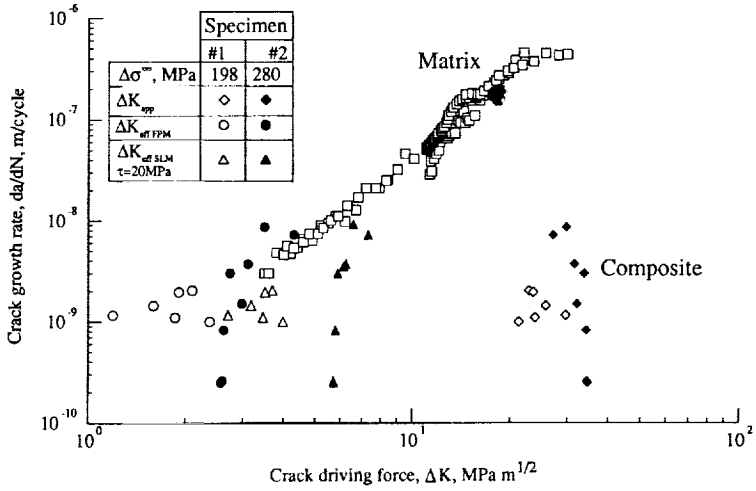

Figure 8.–Corrected FCG data for a bridged composite in relation to the unreinforced matrix alloy FCG data.

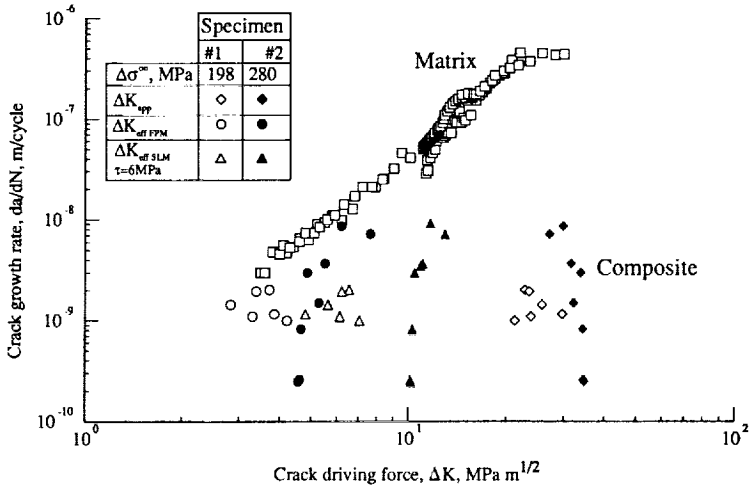

Figure 9.–Crack growth data in terms of the reformulated ΔK_{eff} parameter (eq. 12).

NASA
National Aeronautics and Space Administration

Report Documentation Page

1. Report No.	2. Government Accession No.	3. Recipient's Catalog No.
NASA TM - 104355		

4. Title and Subtitle	5. Report Date
Modeling of Crack Bridging in a Unidirectional Metal Matrix Composite	May 1991
	6. Performing Organization Code

7. Author(s)	8. Performing Organization Report No.
Louis J. Ghosn, Pete Kantzos, and Jack Telesman	E - 6142
	10. Work Unit No. 510 - 01 - 50

9. Performing Organization Name and Address	11. Contract or Grant No.
National Aeronautics and Space Administration Lewis Research Center Cleveland, Ohio 44135 - 3191	
	13. Type of Report and Period Covered Technical Memorandum

12. Sponsoring Agency Name and Address	14. Sponsoring Agency Code
National Aeronautics and Space Administration Washington, D.C. 20546 - 0001	

15. Supplementary Notes

Louis J. Ghosn, Sverdrup Technology, Inc., Lewis Research Center Group, 2001 Aerospace Parkway, Brook Park, Ohio 44142. Pete Kantzos and Jack Telesman, NASA Lewis Research Center. Responsible person, Louis J. Ghosn, (216) 433 - 3249.

16. Abstract

The effective fatigue crack driving force and crack opening profiles were determined analytically for fatigue tested unidirectional composite specimens exhibiting fiber bridging. The crack closure pressure due to bridging was modeled using two approaches; the fiber pressure model and the shear lag model. For both closure models, the Bueckner weight function method and the finite element method were used to calculate crack opening displacements and the crack driving force. The predicted near crack tip opening profile agreed well with the experimentally measured profiles for single edge notch SCS-6/Ti-15-3 metal matrix composite specimens. The numerically determined effective crack driving force ΔK_{eff} was calculated using both models to correlate the measured crack growth rate in the composite. The calculated ΔK_{eff} from both models accounted for the crack bridging by showing a good agreement between the measured fatigue crack growth rates of the bridged composite and that of unreinforced, unbridged titanium matrix alloy specimens.

17. Key Words (Suggested by Author(s))	18. Distribution Statement
Fiber bridging; Metal matrix; Shear-lag; Closure model; Fatigue crack growth; Crack opening; Composite	Unclassified - Unlimited Subject Category 39

19. Security Classif. (of the report)	20. Security Classif. (of this page)	21. No. of pages	22. Price*
Unclassified	Unclassified	22	A03

NASA FORM 1626 OCT 86

*For sale by the National Technical Information Service, Springfield, Virginia 22161